

# An Innovative fuzzy logic controller for power quality Optimization using MLI-UPQC with solar PV-BESS

D. Tejakrishna <sup>1</sup> Mr. Ramu<sup>2</sup>

<sup>1</sup>M.Tech Student, Department of Electrical and Electronics Engineering, Quba College of Engineering and Technology, Venkatachalam, Nellore, Andhra Pradesh, India

<sup>2</sup>Head of The Department , Department of Electrical and Electronics Engineering, Quba College of Engineering and Technology, Venkatachalam, Nellore, Andhra Pradesh, India

## ABSTRACT

This research work presents a battery energy storage system (BESS) for a solar photovoltaic energy-powered multilevel inverter-unified power quality conditioner (UPQC) with fuzzy logic controller (FLC). Using this new structure helped to solve the difficulties with the distribution system's power quality (PQ). Shunt and series controllers aid in UPQC compensation, is connected to the point of common coupling (PCC) in the distribution system. Here, two level series and shunt voltage converters are replaced with a five level cascaded H-bridge MLI. The two level series and shunt voltage converters are replaced by five level cascaded H-bridge MLIs. The system stability and power quality improved more when compared to the conventional two level inverter and PI controller arrangement for UPQC. The complete proposed system is implemented and tested using MATLAB/SIMULINK software. Here, the simulation results for the FLC-MLI-PV-BESS-UPQC and PI-2LVSI-PV-BESS-UPQC are also contrasted.

Keywords: - BESS, MLI, PV, UPQC, FLC, VSI.

## Article Info

Volume 9, Issue 4

Page Number : 643-656

## Publication Issue

July-August 2022

## Article History

Accepted : 05 August 2022

Published : 29 August 2022

## I. INTRODUCTION

Due to industrial growth and population increases, required more quality power to maintain system stability. Now a days all are focused on renewable energy sources (RES) to meet required power demand. But the main problem is power quality issues in existing transmission system to inter connect these RES [1]. More connected loads are non-linear and unbalanced loads causes' disturbance in supplied

power from distribution system. To overcome these drawbacks, different types of filter technologies are implemented [2]. In filter technologies, active filters gain more popularity to reduce power quality issues in distribution systems. Among active filters, flexible alternating current transmission system (FACTS) gain every one attention to improve power quality and maintain system stability in exiting transmission system. But more power quality problems arises at distribution side. So, distribution FACTS (DFACTS)

technologies implemented in distribution side to overcome these drawbacks. Among all DFACTS, distributed static synchronous compensator (DSTATCOM) gain more popularity to improve power factor in the distribution system [3]. To improve voltage stability employed dynamic voltage restorer's (DVR) are used to improve different voltage issues [4]. The system oscillate and disturbed due to voltage, current and power factor problems in distribution system. so, more researchers focused on these issues and investigated hybrid facts device i.e., combined controller. To reduce voltage related problems and current related problems, the combined controller gives best solution i.e., unified power quality conditioner (UPQC) [5]. But these FACTS devices focused on power quality issues, not suitable to provide continuity in power supply. There is no power supply, the FACTS devices operation is ideal. So, to overcome this problem investigated photovoltaic (PV) connected FACTS devices [6-8]. The PV connected series and shunt FACTS devices are implemented to improve power quality as well as continuity in power supply [9]. To overcome power quality issues with continuity power supply lot of research work is going, PV connected DVR and PV connected DSTATCOM implemented in distribution system to overcome power quality issues along with power interruptions [10-15].

## II. Description of the system

The configuration of the UPQC and the PV energy storage system (ESS) is shown in Figure 1. A three phase system is added to the PV-BESS-based UPQC system. A DC-Link Split Capacitor connects the shunt APF compensators and UPQCs from the PV-BESS series. The DC-Link is in contrast to the PV-BESS. The DC-connect and PV are connected by a lift converter. A buck-support converter is used to link the BESS to the DC interface. A regulated voltage source is used by the series compensator to operate, which reduces the voltage's harmonics,

interruptions, swells, and sags. On the other side, the shunt compensator suppresses the harmonic current of the load. The APF compensator is connected employing both the shunt and series interfacing inductors.

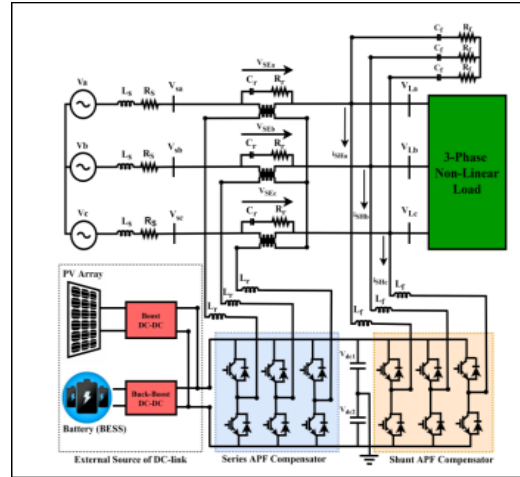


FIGURE 1. Circuit diagram of FLC-PV-BESS-MLI-UPQC

A ripple filter is used to remove the harmonics that are created by the converter switching process. A series injection transformer is used by the series compensator to inject electricity into the grid. In this work, a three-phase non-linear load is employed. Before beginning the PV-BESS-UPQC design process, precise measurements of the PV array, split capacitor, reference voltage of the DC-link, etc. are taken. The shunt compensator reduces current harmonics and regulates the peak output power of PV arrays.

### 1. PV-BESS-UPQC

For constructing UPQC systems based on solar and BESS, the system model in Fig.2 has included the buck-boost, boost, and controllers. The BESS and the DC Link capacitor of the buck-boost converter work together to improve the UPQC's efficiency and reliability while reducing power quality problems. The model depicts the real source of power as (7).

$$P_{total} = P_{pv} + P_{BESS} - P_{LoadDC-link} \quad (1)$$

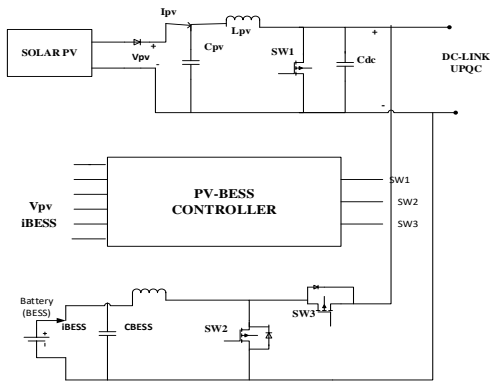


FIGURE 2. Block diagram of PV-BESS-UPQC

2. Solar PV system:

The "Simulink" library was utilised to get the photovoltaic model that was employed in this study. The PV model consists of parallel strings of PV modules. The primary goal of the design of this PV module was to obtain the necessary  $I_{pv}$ ,  $V_{pv}$ , and  $P_{pv}$  ratings (current, voltage, and power). A PV module's efficiency can be raised by using MPPT under particular irradiance and temperature conditions. The connected DC-DC boost converter's duty cycle will enable the MPPT algorithm to produce pulses. Different categories have been developed for MPPT techniques. However, this study work perturb and observe (P & O) into consideration for the objectives of this implementation. Because tracking the maximum power in this research is more accurate. The flowchart below is used to implement the P & O algorithm (3).

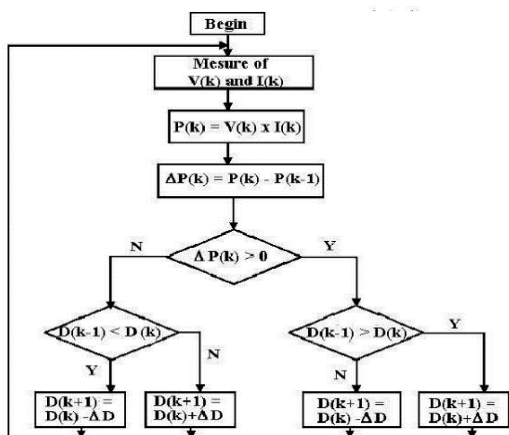


FIGURE 3. P&O MPPT (producing duty cycle for boost converter)

Figure 4 depicts the controller for the step-up converter (DC-DC boost converter) that increases the power of the PV system. A DC voltage error,  $V_{DC}$ , is sent to the DC-DC boost converter's controller, which then turns on. By comparing the voltage to the reference voltage,  $V_{ref}$ , which is set at 700V, the voltage inaccuracy is determined. The simultaneous DC-DC Boost converter output DC voltage  $V_{DC}$  serves as the reference voltage. In order to lower  $V_{DC}$ , error a PI controller is then used to approximate  $V_{DC}$ , error (t) (t). Mathematically, the following may be determined about the approximation from (8) and (9):

$$V_{DC,error} * = K_{p,1} (V_{DC,error}(t)) . dt + K_{i,1} \int_0^t (V_{DC,error}(t)) . dt \quad (2)$$

$$V_{DC,error}(t) = V_{ref} + V_{DC}(t) \quad (3)$$

Where the PI1 controller's proportional and integral gains are represented, respectively, by the two constants  $K_{P1}$  and  $k_{i1}$ . The numbers are 0.1 and 0.1, respectively. This PV-BESS architecture's battery life may be reduced by overcharging. The solution to this problem uses the topology of a DC-DC step-up converter to stabilize the battery system and prevent overcharging.

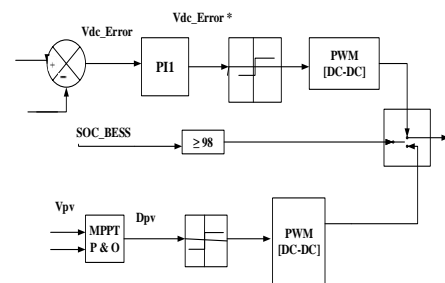


FIGURE 4. Simulink control topology for step up converter

3. BESS

For BESS modelling, batteries are commonly constructed from one or more batteries connected either in parallel or series. The majority of battery models are often developed from the electrical circuit models, which are the basis for classifying battery models in general. For instance, integrating current enhances the battery's Peukert's equation model. An electrochemical model is also the Shepherd equation. The usage of a mathematical model in this work is made possible by effective software like MATLAB/SIMULINK. Due to their high power density, low maintenance requirements, and high energy output, lithium-ion batteries are the ones that garner the most attention among all of these batteries.

**4. PV-BESS optimization method**

Figure 5 shows a bidirectional Buck-Boost DC-DC controller with integrated internal and exterior charging and discharging control loops.

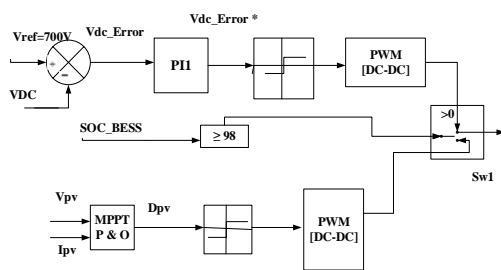


**FIGURE 5. BESS optimizing technique**

The frequency is kept stable by active power supplied by an external control that is set up appropriately and has a frequency droop. A voltage control loop for system voltage stability and a current control loop for adjusting the filter output current for quick dynamic response make up the internal control loop. To determine the current reference voltage, the reference DC Link voltage and the measured PV dc link voltage ( $V_{DC}$ ) are contrasted ( $V_{DC, ref}$ ). The voltage controller's outer loop then receives the difference once it has been sent by the PI2 controller. The following equations represent the method mathematically: (10) and (11)

$$V_{DC,error}(t) = V_{ref}V_{DCref} * (t) \quad (4)$$

$$i_{t,ref} = K_{P,2} (V_{DC,error}(t)) + K_{i,2} \int_0^t (V_{DC,error}(t)) dt \quad (5)$$

Where the proportional and integral gains of the PI2 controller are indicated by the two fixed numbers  $kp2$  and  $ki2$ , respectively. 3077 and 1.477 are the values, respectively. A voltage control loop for system voltage stability and a current control loop for adjusting the filter output current for quick dynamic response make up the internal control loop. To determine the current reference voltage, the reference DC Link voltage and the measured PV dc link voltage ( $V_{DC}$ ) are contrasted ( $V_{DC, ref}$ ).The voltage controller's outer loop then receives the difference once it has been sent by the PI2 controller.

**5. Grid synchronization with proposed topology**

The system voltage is maintained by a voltage control loop, and the filter output current is adjusted by a current control loop for quick dynamic response. By comparing the measured PV dc link voltage ( $V_{DC}$ ) with the reference DC Link voltage, the current reference voltage is determined ( $V_{DC, ref}$ ). The voltage controller's outer loop receives the difference once the PI2 controller sends it.

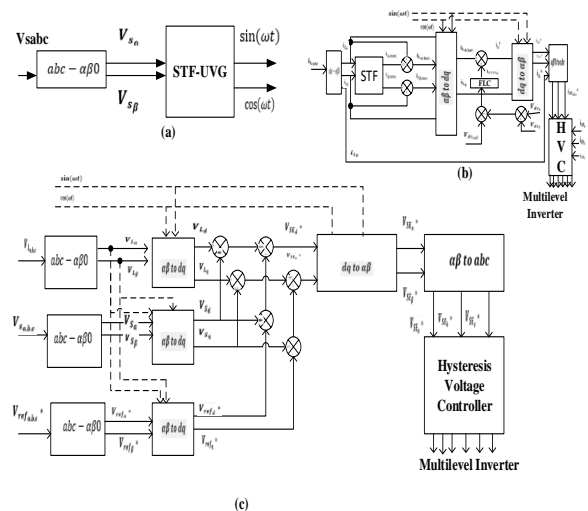


**FIGURE 6. FLC control topology block diagram (A) block diagram of STF-UVG (B) Shunt controller-control technique (C) Series controller-control technique**

There would only be evaluation of two phases in the - domain. When supply voltage is altered, fundamental and harmonic component production might occur. The connection is shown in (12).

$$\begin{matrix} V_{sa} \\ V_{sb} \end{matrix} = \begin{matrix} V_{sa(fund)} \\ V_{sb(fund)} \end{matrix} + \begin{matrix} V_{sa(har)} \\ V_{sb(har)} \end{matrix} \quad (6)$$

The STF method is used to extract the important elements. The harmonic components of the system can be suppressed using this method. The extraction quality is enhanced as a result, and synchronization stages are eliminated more precisely.

$$\begin{matrix} V_{sa(fund)S} \\ V_{sb(fund)S} \end{matrix} = \frac{K_1}{S} \begin{bmatrix} V_{sa} S - V_{sa(fund)S} \\ V_{sb} S - V_{sb(fund)S} \end{bmatrix} + \frac{2\pi f_{c1}}{S} \begin{bmatrix} -V_{sb(fund)S} \\ V_{sa(fund)S} \end{bmatrix} \quad (7)$$

K1 will stand for the constant gain parameter, and fc1 will stand for the frequency at the cut-off region. The range of the K1 rating is thought to be between 20 and 80, whereas the system frequency determines the fc1 rating. In this project, it is expected that K1 will have a rating of 20 Hz and fc1 will have a rating of 50 Hz. A method known as UVG will be used to circumvent the functioning of a phase locked loop element (PLL), and in the UPQC topology, the phases of synchronization will be effectively and efficiently generated while the supply voltage distortions are still taking place.

**6. Series controller**

STF-frequency One can use phase data and UVG analysis to The reference voltage signal Vref, abc, which is connected in three phases, can be computed in the abc-domain using the frequency and phase data of STF-UVG, as described in the paragraph below (13) The maximum peak voltage magnitude, also known as Vm, max peak, is calculated using the peak amplitude of the fundamental load voltage. The reference and supply voltages, where the d-frames represent the maximum amplitude load reference voltage and the q-frames the supply voltage, must be in phase with the PCC Zero.

$$\begin{matrix} V_{refa}^* \\ V_{refb}^* \\ V_{refc}^* \end{matrix} = V_{m_{max-peak}} \begin{bmatrix} \sin(\omega t) \\ \sin(\omega t - \frac{2\pi}{3}) \\ \sin(\omega t + \frac{2\pi}{3}) \end{bmatrix} \quad (8)$$

By utilising this STF-UVG, it is possible to extract the voltage supply at PCC for the fundamental component's distorted and synchronized phase creation, and the acquired frequency is then used to construct the dq-frames' axis of reference. In the dq-frames, the reference voltage signal is acquired with only two phases and the Park transformation matrix.

**Shunt controller**

The harmonic component of the load current is extracted using the suggested STF on -domain. The fundamental and harmonic parts of the load current iL signal can be distinguished by concentrating on the -domain. K1 is anticipated to have a rating of 20 Hz and fc1 to have a rating of 50 Hz in this project. In this controlled topology, Dq-axis currents were employed. Equation (9) shows how this results in the transformation into a dq-frame:

$$i_{lq} = i_{l\alpha} \cos(\omega t) + i_{l\beta} \sin(\omega t) \quad (9)$$

Transformation is not needed in the 0-domain. The magnitude of the fundamental current at the load side is represented by the d-DC frame component, whereas the magnitude of the harmonic current is represented by the oscillating AC frame component.

The error is then found by lowering the PI controller error e1 (t) between the reference dc-link voltage Vdc and total instantaneous dc-link voltage, which is provided by Dc (15) and (16).

$$i_{errordc} = k_{p,4} e_1(t) + k_{i,4} \int_0^t e_1(t) dt \quad (10)$$

$$e_1(t) = V_{dc,ref} - (V_{Cap1}(t) + V_{Cap2}(t)) \quad (11)$$

The PI4 controller's integral gain is represented by Ki4=2, kp, 4=0.3, represents the proportional gain. The following figures can be used to calculate the reference current if grid in the frame of dq:

$$i_{Ld}^* = i_{Ld(har)} - i_{errordc} \quad (12)$$

The current signals  $i_{L,d}$  and  $i_{L,q}$  are then converted into the abc domain by adding grid currents. By combining (18) and (19), the reference current  $i_{sH, abc}$  is produced. The comparison between the reference supply currents and measured supply currents is necessary for the shunt converter to generate the gate pulses.

$$\begin{bmatrix} i_{Ld}^* \\ i_{L\beta}^* \end{bmatrix} = \begin{bmatrix} \sin(\omega t) & \cos(\omega t) \\ -\cos(\omega t) & \sin(\omega t) \end{bmatrix} \begin{bmatrix} i_{Ld} \\ i_{Lq} \end{bmatrix} \quad (13)$$

$$\begin{bmatrix} i_{SH\alpha}^* \\ i_{SH\beta}^* \\ i_{SHc}^* \end{bmatrix} = \sqrt{\frac{2}{3}} \begin{bmatrix} 1 & 0 \\ -\frac{1}{2} & \frac{\sqrt{3}}{2} \\ -\frac{1}{2} & -\frac{\sqrt{3}}{2} \end{bmatrix} \begin{bmatrix} i_{L\alpha}^* \\ i_{L\beta}^* \end{bmatrix} \quad (14)$$

**7. MLI-FLC:**

The concept of multilevel inverters extends back to 1975. The necessary for the future behind the development of multilevel inverters was the three level inverter. In order to meet the system's needs, various topologies have developed since the introduction of multilayer inverters. The power semiconductor switches known as multilevel inverters/converters, which have the lowest dc voltage sources, convert power by integrating a voltage waveform that looks like a staircase.

- **Proposed MLI**

A cascaded H-bridge inverter was used in this experiment. A cascaded H-bridge MLI's structural diagram is shown below. An H-bridge is built by coupling a single phase full-bridge inverter to a number of DC sources. By connecting a DC source to the output of an AC current, S1, S2, S3, and S4 can all be switched in this configuration. An inverter is the outcome of this coupled topology. The three voltage types +Vdc, 0Vdc, and -Vdc can thus be produced by each inverter level. S1 and S2 switches will activate +Vdc, whilst S2 and S3 switches will activate -Vdc. When each of the four switches is in the ON position, there is no voltage at the output. Several full-bridge inverter levels' injecting current

outputs can be connected in series to create a voltage waveform that nearly matches the inverter output. The output phase voltage level of a cascaded H-bridge inverter is denoted by the notation  $m=2s+1$ . Since it equals all of the circuit's voltages, the Van is frequently referred to as the phase voltage Van: -  $V_{an}=V_{a1}+V_{a2}+V_{a3}+V_{a4}+V_{a5}$ . Detailed information on the 11-level H-Bridge MLI is shown in Figure 7 below.

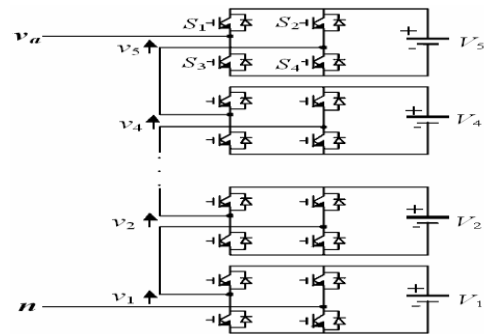


**Fig 7. Circuit diagram of CH-MLI**

**a) FLC:**

The Fuzzy Logic method is a sophisticated mathematical approach used to solve simulation problems with a large number of input and output variables. Similar to Boolean algebra, the Fuzzy Logic Controller (FLC) can supply critical and specialized logics. The basic concepts of fuzzy logic are summarized in this study. These days, control systems are frequently described using stochastic models, mathematical models based on mathematical logic, and mathematical models based on physical principles. Such a model often makes an effort to determine how to get from a given challenge to an appropriate calculated exemplary. Today's sophisticated computer technology makes it unquestionably conceivable, but sustaining such systems is still somewhat challenging [14–[15]. Figure

10 depicts the fuzzy inference engine, fuzzy rule matrix, defuzzification interface, and fuzzification interface as the four primary components of the FLC system.

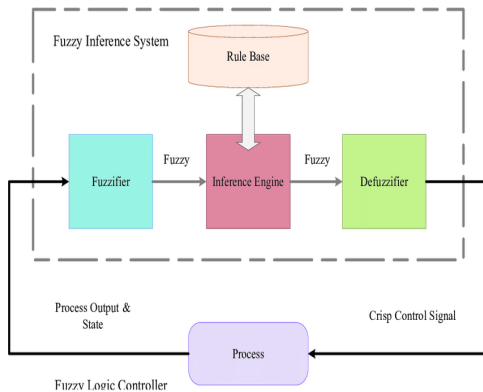


Figure 8. Block diagram of FLC

The membership operations of the fuzzy logic controller are shown in the image below. Figure (9) displays the outcome after taking into account the two inputs of error and change in error (11).

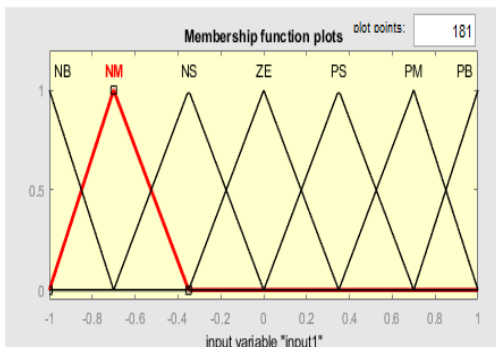


Figure (9): FLC input-1 (error) membership functions

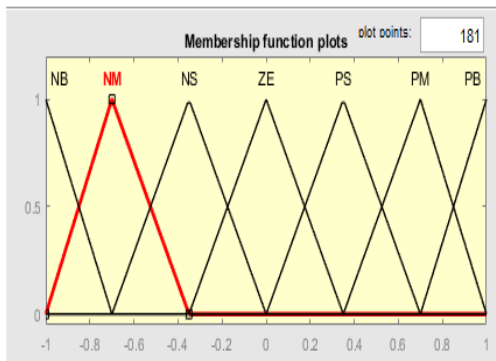


Figure (10): FLC input-2 (change in error) membership functions

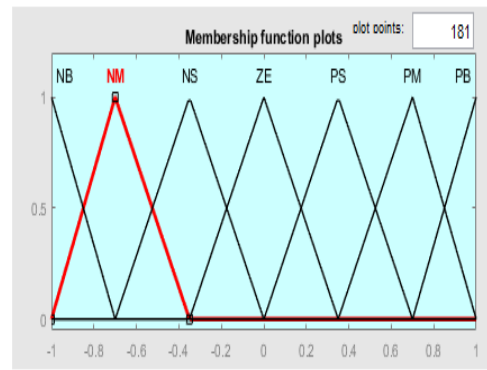


Figure (11): FLC output membership function

Table 2: FLC rule base

CE/E	NB	NM	NS	ZE	PS	PM	PB
NB	NB	NB	NB	NB	NM	NS	ZE
NM	NB	NB	NB	NM	NS	ZE	PS
NS	NB	NB	NM	NS	ZE	PS	PM
ZE	NB	NM	NS	ZE	PS	PM	PB
PS	NM	NS	ZE	PS	PM	PB	PB
PM	NS	ZE	PS	PM	PB	PB	PB
PB	ZE	PS	PM	PB	PB	PB	PB

The above table consists of the 7x7=49 rules, whereas

Positive Small=PS; Positive Medium=PM; Positive Big=PB; Negative Big=NB; Negative Medium=NM; Negative Small=NS; Zero Error=ZE.

### III. SIMULATION RESULTS:

#### FLC-MLI:

##### Case-1:

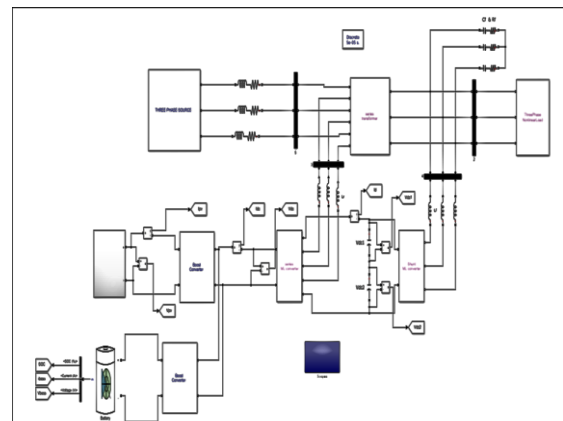


**Figure 12: case-I simulation diagram**

The above simulation diagram shows the case-I proposed FLC-PV-BESS-UPQC for PQ optimization. Here boost converter, bi-directional converter and UPQC are controlled by three different control techniques. MPPT topology employed for boost converter controlling, PI controller employed for bi-directional converter and FLC employed for UPQC. After proposed structure completed, run the simulation model and taken the executed results.

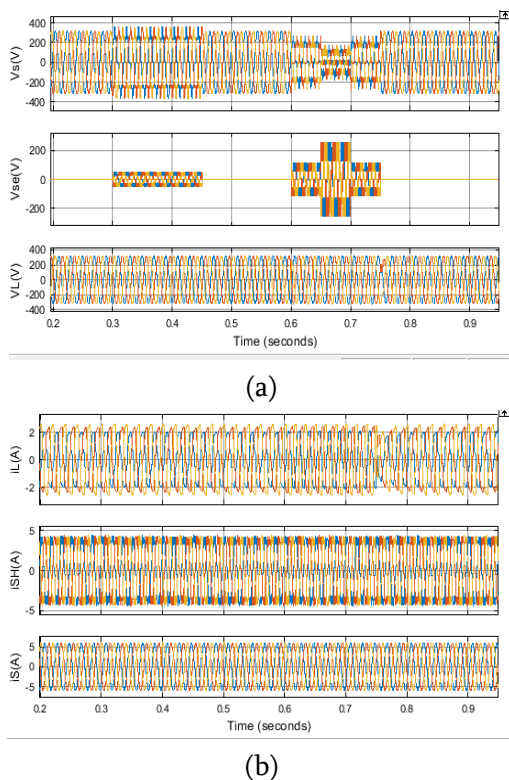


**Fig 13 (a) Grid ,series controller injected and load Voltage (b) Grid, shunt controller injected and load current**

The above figure 13 (a) shows the voltage waveforms of grid, series controller injected and load. Similarly figure 13(b) shows the grid shunt controller injected load current in case-I. In case-I the proposed system connected to a non-linear load with variable irradiation value.

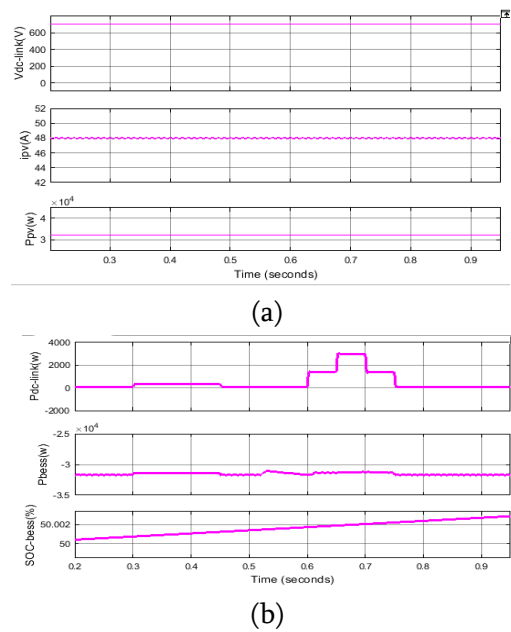


**FIGURE 14. (a) Battery soc, power of dc-link, battery power (b) PV power, current and dc link voltage**

The above figure 14 (a) shows the voltage waveforms of grid, series controller injected and load. Similarly figure 14(b) shows the grid shunt controller injected load current in case-I. In case-I the proposed system connected to a non-linear load with variable irradiation value.

**Case-ii**

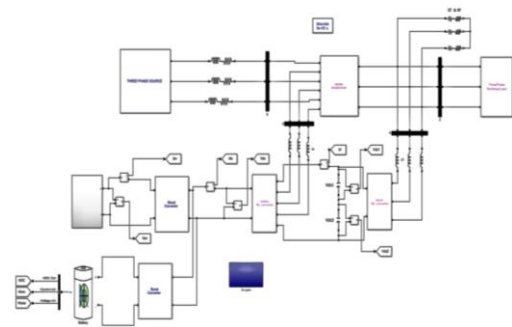


**Fig 15: Structure of FLC-PV-BESS-MLI-UPQC (case-II)**

The above simulation diagram shows the case-II proposed FLC-PV-BESS-UPQC for PQ optimization. Here boost converter, bi-directional converter and UPQC are controlled by three different control techniques. MPPT topology employed for boost converter controlling, PI controller employed for bi-

directional converter and FLC employed for UPQC. After proposed structure completed, run the simulation model and taken the executed results.

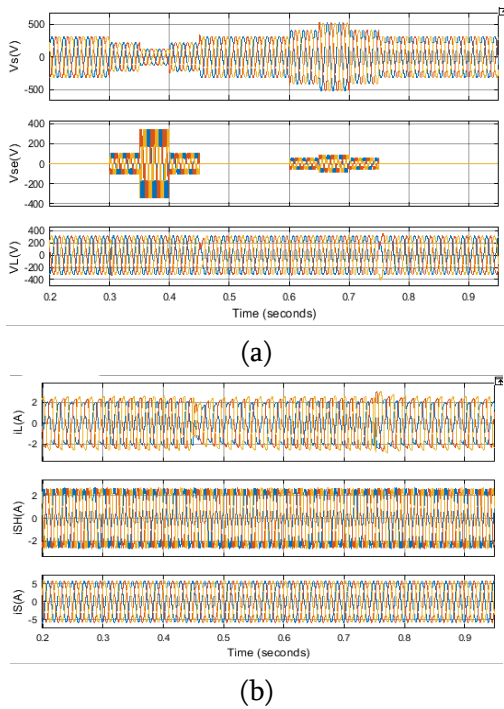


**FIGURE Fig 16 (a) Grid ,series controller injected and load Voltage (b) Grid, shunt controller injected and load current**

The above figure 16 (a) shows the voltage waveforms of grid, series controller injected and load. Similarly figure 16(b) shows the grid shunt controller injected load current in case-II. In case-II the proposed system connected to a non-linear load with voltage sag and swell condition.

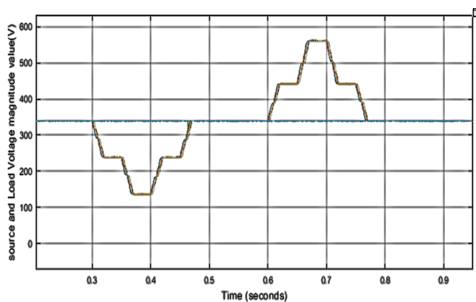


**FIGURE 17. Voltage deviation in case-II**  
**The above figure depicts the voltage deviation in case-II**

The above figure shows the deviation in voltage at PCC under case-II. In case-II proposed system

connected to non-linear load with voltage sag and swell condition.

**THD analysis of FLC-PV-BESS-MLI and PI-PV-BESS-2L VSI:**

**CASE-I**

parameter	PI-2L VSI (%)	FLC-MLI (%)
Ig-supply voltage harmonics	2.51	1.36
Ig-supply current harmonics with sag	2.48	1.36
Vg	0.52	0.52

The above shows the THD comparison between conventional method and proposed method in case-I. In 2LVSI and FLC-MLI UPQC the grid current THD is 2.51 and 1.36 respectively under supply voltage harmonics. Similarly grid current THD with sag condition is 2.48 and 1.36 respectively. And also grid voltage THD is 0.52 in conventional and proposed method.

**CASE-II**

**Balanced condition**

Parameter	PI-2L VSI (%)	FLC-MLI (%)
Ig-swell condition	2.51	0.65
Ig-sag condition	2.53	0.64
Vg	0.52	0.52

The above shows the THD comparison between conventional method and proposed method in case-II balanced condition. In 2LVSI and FLC-MLI UPQC

the grid current THD is 2.51 and 0.65 respectively under supply voltage harmonics. Similarly grid current THD with sag condition is 2.53 and 0.64 respectively. And also grid voltage THD is 0.52 in conventional and proposed method.

**CASE-II**

**Unbalanced condition**

parameter	PI-2L VSI (%)	FLC-MLI (%)
Ig-sag condition	2.48	1.31
Ig-swell condition	2.48	1.33
Vg	0.53	0.53

The above shows the THD comparison

between conventional method and proposed method in case-II un-balanced condition. In 2LVSI and FLC-MLI UPQC the grid current THD is 2.48 and 1.31 respectively under supply voltage harmonics. Similarly grid current THD with sag condition is 2.48 and 1.33 respectively. And also grid voltage THD is 0.53 in conventional and proposed method.

**IV. Existing System**

In existing we don't have any proper equipment to monitor the patient's health parameters wirelessly. So that a care taker is required continuously in order to measure the health parameters which may affect the care taker also. If the care taker is not aware of or shows any negligence then there is a chance of causing death of the patient. So, there is a need of wireless and long-distance communication.

**Drawbacks:**

- Patient Data is not exchanged Continuously.
- Patient needs to attend for every checkup.
- Critical condition is unknown.

**V. Proposed System**

Main purpose of IoT based system to help healthcare system in case of emergencies. The system self-monitor and able to inform critical situations of patients to the doctors. Sensors signals are sent to Arduino via ESP8266. Here patients body temperature, respiration, movements and heartbeat values are measured using respective sensors and it can be monitored in the cloud database system as well as monitored anywhere in the world using internet source.

**Block Diagram:**

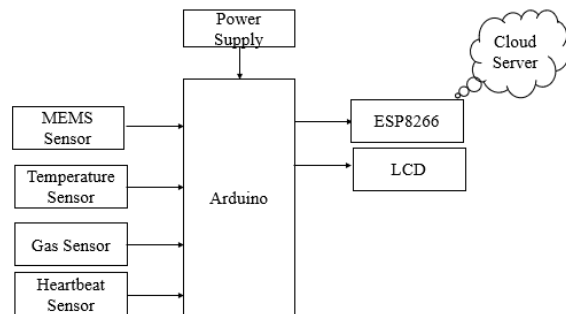


**Fig1: Block Diagram**

**Hardware Requirements**

**Power Supply:**

**Transformer:**



**Fig2: Transformer**

Transformer is a device which reduces A.C current into required D.C current.

**Bridge Rectifier:**



**Fig3: Bridge rectifier**

A diode bridge is a technique of four diodes in a bridge circuit arrangement that provides equal polarity of output for mutually polarity of input. While used in its maximum shared application, for transformation of an alternating-current input into a direct-current output, it is called as a bridge rectifier.

**Capacitor:**



**Fig4:Capacitor**

A capacitor could be a passive two terminal electrical component that stores current in a electric field. The result of this can be termed as capacitance.

**Regulator:**

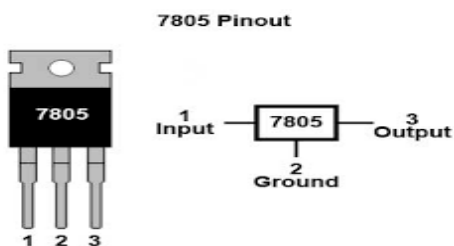


**Fig5: Regulator**

A voltage regulator IC keeps the output voltage at a continuous value. 7805 IC is one of the IC of 78xx family. It maintains fixed linear regulators which is used to maintain fluctuations.

**Arduino:**

Arduino uno is a microcontroller board which inbuilt has an IC that is ATmega328P which is Main Microcontroller. In this we have 14 digital pins, 6

Analog Pins, 16MHz Crystal Oscillator and a Reset Button.



**Fig6: Arduino**

**ESP8266 WIFI Module:**

The ESP8266 WiFi module is a self-contained SOC with integrated TCP/IP protocol stack that can give any microcontroller access to your WiFi network. The ESP8266 is capable of either hosting an application or offloading all WiFi networking functions from another application processor.

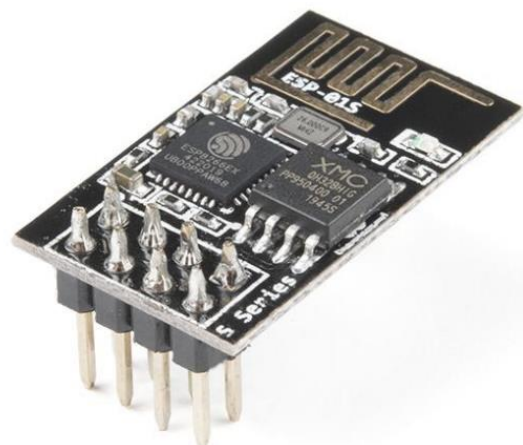


**Fig7: ESP8266 WIFI Module**

**Relay:**

Relay is electromagnetic switch that open or close the switches electrically or electromechanically. Relay is mostly used to switch smaller circuits.



**Fig8: Relay**

**Gas Sensor:**

MQ2 gas sensor can be used to detect the presence of LPG, Propane and Hydrogen, also could be used to detect Methane and other combustible steam, it is with low cost and suitable for different application. Sensor is sensitive to flammable gas and smoke.



**Fig9: Gas Sensor**

**MEMS Sensor:**

MEMS are slight expense, and high exactness inertial sensors and these are utilized to serve a broad scope of modern applications. This sensor utilizes a chip-based innovation specifically micro-electro-mechanical-system. These sensors are utilized to distinguish as well as measure the outside enhancement like tension and strain.

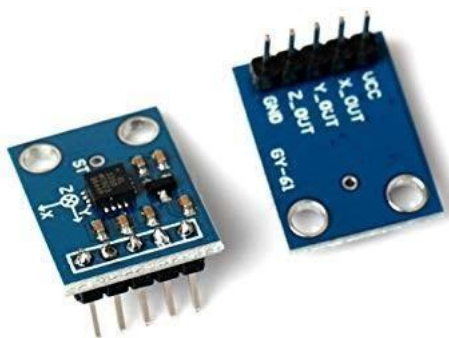


**Fig10: MEMS Sensor**

**LM35 Temperature Sensor:**

The LM35 series are accuracy incorporated circuit temperature sensors, whose resultvoltage is straightly corresponding to the Celsius (Centigrade) temperatureIts output is 10 MilliVolts per degree

centigrade. So if the output is 310 mV then temperature is 31 degree C. It has a range of -55 to +150°C temperature range. LM35 is a popular and low-cost temperature sensor. To use the sensor simply connect the Vcc to 5V, GND to Gnd and the Out to one of the ADC (analog to digital converter channel). The output linearly varies with temperature.

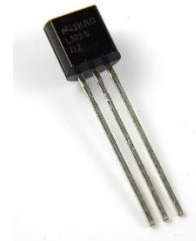


**Fig11: Temperature Sensor**

**Heartbeat Sensor:**

Heartbeat Sensor is an electronic device that is utilized to scale thepulse for example speed of the heartbeat. Observing internal heat level, pulse and bloodpressure are the fundamental things that we really do to keep us solid.



**Fig12: Heartbeat Sensor**

**LCD:**

In LCD 16x2, the term LCD represents Liquid Crystal Display that utilizes a plane board show innovation, utilized in screens of PC screens and TVs, cell phones, tablets, cell phones, and so forth. Both the showcases like LCD and CRTs appear to be identical yet their activity is unique. Rather than electrons diffraction at a glass display, a liquid crystal display show has a backdrop illumination that gives light to every pixel

that is organized in a rectangular organization.



Fig13: LCD

## VI. CONCLUSION

The entire proposed PV-BESS-UPQC system with FLC and conventional PI controller implemented in simulation software. By testing the proposed system, it has been proven that the FLC and MLI structure for UPQC increased the system stability and power quality more than the conventional two-level inverter and PI controller setup. The comparative results between the suggested fuzzy logic controller for PV-BESS-UPQC and the conventional PI controller for PV-BESS-UPQC reveal the best method for enhancing power quality in the distribution system. For instance, the FLC-MLI structure for PV-BESS-UPQC.

## VII. REFERENCES

### Software Requirements

#### Arduino IDE:

The Arduino IDE software is an open-source software, where we can have the example codes for the beginners. In the Present world there are lot of versions in the Arduino IDE in which present usage is Version1.0.5. It is very easy to connect the PC with Arduino Board.



## VI. Advantages

1. Monitoring the Patient Continuously.
2. They can easily communicate with us.

## VII. Applications

1. Used in the hospitals
2. Patients at home

- [1]. M S. K. Khadem, M. Basu, and M. Conlon, "Power quality in grid connected renewable energy systems: Role of custom power devices," 2010.
- [2]. Y. Zhao. (2016, November 11). Electrical Power Systems Quality. Available: <http://best.eng.buffalo.edu/Research/Lecture%20Series%202013/Power%20Quality%20Intro.pdf>
- [3]. M. Badoni, A. Singh, and B. Singh, "Variable forgetting factor recursive least square control algorithm for DSTATCOM," IEEE Trans. Power Del., vol. 30, no. 5, pp. 2353–2361, Oct 2015.
- [4]. V. Khadkikar, "Enhancing electric power quality using UPQC: A comprehensive overview," IEEE Trans. Power Electron., vol. 27, no. 5, pp. 2284–2297, May 2012.
- [5]. A. Teke, L. Saribulut, and M. Tumay, "A novel reference signal generation method for power-quality improvement of unified powerquality conditioner," IEEE Trans. Power Deliv., vol. 26, no. 4, pp. 2205–2214, 2011.
- [6]. V. G. Kinhal, P. Agarwal, and H. O. Gupta, "Performance investigation of neural-network-based unified power-quality conditioner," IEEE

- Trans. Power Deliv., vol. 26, no. 1, pp. 431–437, 2011.
- [7]. Libo, Z. Zhengming, and L. Jianzheng, "A single-stage three-phase grid-connected photovoltaic system with modified MPPT method and reactive power compensation," IEEE Trans. Energy Convers., vol. 22, no. 4, pp. 881–886, Dec. 2007.
- [8]. [M. Davari, S. Ale-Emran, H. Yazdanpanahi, and G. Gharehpetian, "Modeling the combination of UPQC and photovoltaic arrays with multi-input single-output dc-dc converter," in IEEE/PES Power Systems Conference and Exposition, 2009. PSCE '09., March 2009, pp. 1–7.
- [9]. B. G. Campanhol, S. A. O. Da Silva, A. A. De Oliveira, and V. D. Bacon, "Power flow and stability analyses of a multifunctional distributed generation system integrating a photovoltaic system with unified power quality conditioner," IEEE Trans. Power Electron., vol. 34, no. 7, pp. 6241–6256, 2019
- [10]. Czarnecki, "Constraints of instantaneous reactive power p-q theory," IET Power Electronics, vol. 7, no. 9, pp. 2201–2208, September 2014
- [11]. S. B. Karanki, N. Geddada, M. K. Mishra, and B. K. Kumar, "A modified three-phase four-wire UPQC topology with reduced DClink voltage rating," IEEE Trans. Ind. Electron., vol. 60, no. 9, pp. 3555–3566, 2013.
- [12]. A. Teke, L. Saribulut, and M. Tumay, "A novel reference signal generation method for power-quality improvement of unified powerquality conditioner," IEEE Trans. Power Deliv., vol. 26, no. 4, pp. 2205–2214, 2011.
- [13]. V. G. Kinhal, P. Agarwal, and H. O. Gupta, "Performance investigation of neural-network-based unified power-quality conditioner," IEEE Trans. Power Deliv., vol. 26, no. 1, pp. 431–437, 2011.
- [14]. K. K. Gupta, A. Ranjan, P. Bhatnagar, L. K. Sahu and S. Jain, "Multilevel Inverter Topologies With Reduced Device Count: A Review," in IEEE Transactions on Power Electronics, vol. 31, no. 1, pp. 135–151, Jan. 2016
- [15]. Elango R. Subramanian Venugopal Manikandan Krishnan Ramakrishnan. Department of Electrical and Electronics Engineering, Coimbatore Institute of Technology, Civil Aerodrome Post, Coimbatore 641-014, Tamil Nadu, India.

#### Authors profile :



DHANIKELA TEJAKRISHNA  
currently Pursuing Post Graduation  
at QUBA COLLEGE OF  
ENGINEERING AND  
TECHNOLOG



A. Ramu received post graduation  
degree specialisation of electrical  
power systems in N.B.K.R.I.S.T,  
Vidyanagar, and presently working  
as assistant professor in EEE  
Department At QUBA College Of Engineering  
And Technology Venkatachalam, Nellore A.P

#### Cite this article as :

D. Tejakrishna, Mr. Ramu, "An Innovative fuzzy logic controller for power quality Optimization using MLI-UPQC with solar PV-BESS", International Journal of Scientific Research in Science and Technology (IJSRST), Online ISSN : 2395-602X, Print ISSN : 2395-6011, Volume 9 Issue 4, pp. 643-656, July-August 2022.

Journal URL : <https://ijsrst.com/IJSRST2294110>